Analytical Modeling of Temperature Distribution in Metal Cutting: Finite Element Approach.

Onyechi, Pius C[1]., Oluwadare, Benjamin S[2]., Obuka, Nnaemeka S.P[1].(Corresponding Author),

[1]*Department of Industrial and Production Engineering, Nnamdi Azikwe University, Awka, Nigeria.*
[2]*Department of Mechanical Engineering, Ekiti State University, Ado Ekiti, Nigeria.*

ABSTRACT: *This work covers analysis of the effect of temperature distribution in cutting tool life and wear using finite element methods. By modeling the heat intensity at the shear zone as non-uniform, this study tries to obtain cutting forces, stress distributions on the tool rake face and temperature distributions in the deformation zones. In effort to consider the temperature rise on the chip side and also on the tool side along the interface, the heat source method introduced by Jaeger in 1992 was applied. Three dimensional steady heat transfer finite element model problem was designed with boundary conditions that includes specified temperature, insulated condition and active condition. From the experimental, analytical and simulation results; the carbide cutting tool when air cooled maintained constant temperature of 298^0K, but when the cutting tool is insulated the temperature increases rapidly. The FEM analysis and ANSYS simulation show that the cutting tool when its base is convecting has the maximum temperatures of 404^0K and 386.485^0K respectively. The same results were obtained in both cases when the cutting tool base is insulated.*

Keywords: Temperature, Carbide Cutting Tool, Finite Element, Heat Transfer, Simulation, Stress.

I.   INTRODUCTION

Machining is an important manufacturing operation in industry. The purpose of a machining process is to generate a surface having a specified shape and acceptable surface finish, and to prevent tool wear and thermal damage that leads to geometric inaccuracy of the finished part. The thermodynamic approach to the activity at the cutting edge attempts to account for the energy consumed. Research has shown that at least 99 percent of the input energy is converted into heat by deformation of the chip and by friction of the chip and workpiece on the tool [1],[2]. The interface at which the chip slides over the tool is normally the hottest region during cutting. The actual temperature is strongly affected by workpiece material, cutting speed, feed, depth of cut, tool geometry, coolant, and many other variables. Due to the interaction of the chip and tool, which takes place at high pressures and temperatures, the tool will always wear.

The most important part of the work generated during the cutting process is converted into heat [3]. A large number of techniques have been developed to quantify the temperature, which can be classified as intrusive or non-intrusive techniques. Because of the highly nonlinear nature of metal cutting and the complex coupling between deformation and temperature fields, a complete understanding of the mechanics of metal cutting is still lacking and is thus the topic of a great deal of current research.

II.   REVIEW OF LITERATURES

There are three main regions concerned with heating during the cutting process: The primary shear zone where the chip is formed and characterized by high plastic deformation; the secondary deformation zone, where the deformation takes place in the tool-chip interface as a result of friction force; the tertiary deformation zone, where the heat is generated due to friction between tool clearance face and newly generated workpiece surface. Fig, 1 shows generation of heat in metal cutting.
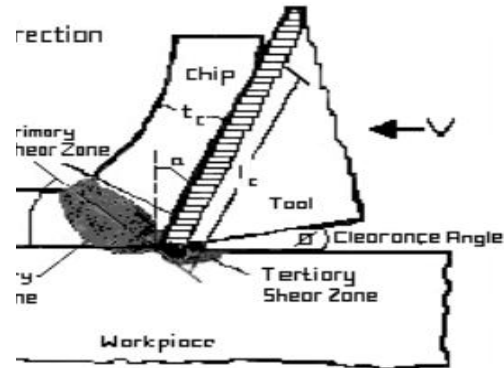
Fig.1: Generation of heat in metal cutting

Numerous methods have also been applied to predict temperatures in machining processes [4],[5],[6],[7] used finite element method and [8] used finite difference method to determine the proportion in which the cutting energy is distributed among the tool, chip and workpiece. Radulescu and Kapoor (1994) [9] developed an analytical model for prediction of tool temperature fields in continuous or interrupted three dimensional cutting processes. The analysis predicts time dependent heat fluxes into the cutting tool, and it only requires the cutting forces as inputs. Pyrometry techniques are often used to study the mechanical behaviour of material because they have many advantages compared to the thermocouple techniques [10]. At the forefront of analytical modeling, based on the moving heat source method, the analytical modeling of steady-state temperature in metal cutting has been presented by [11], [12], and more recently by [13]. In evaluating the combined effects of two heat sources, [13] considered the effect of the primary heat source on the final temperature rise within the tool by introducing an induced stationary rectangular heat source caused by the primary heat source.

The heat source method introduced by [14], [15] is applied in this study. The temperature rises on the chip side and also on the tool side along the interface; thus the tool–chip interface boundary is adiabatic for the tool and the chip respectively. Similarly, the tool–workpiece interface boundary is considered to be adiabatic for the tool and the workpiece respectively. Outeiro et al (2004) [16] developed a 3D dynamic temperature field control models that calculates the temperature of heat sources in the light of tool temperature distribution information. The materials used for machining includes Ti-6Al-V4 and AISI 1008, with varying LN2 coolant jet configurations and then analyzed using finite element technique.

2.1 Temperature Fields in Machining Processes

The temperature of a tool plays an important role in thermal distortion and the machined part's dimensional accuracy, as well as tool life in machining. The most significant factors in tool wear are temperature and the degree of chemical affinity between the tool and the workpiece. Research has shown that at least 99 percent of the input energy is converted into heat by deformation of the chip and by friction of the chip and workpiece on the tool [1],[2]. The interface at which the chip slides over the tool is normally the hottest region during cutting. The actual temperature is strongly affected by workpiece material, cutting speed, feed, depth of cut, tool geometry, coolant, and many other variables [12]. Due to the interaction of the chip and tool, which takes place at high pressures and temperatures, the tool will always wear..

A review of the most common experimental techniques for temperature measurement in metal cutting processes reveals that these techniques can be classified as: direct conduction, indirect radiation, and metallographic. These techniques have been reviewed by [3],[17], and more recently by [13], [18], and [19]. Generally, these techniques include: tool-work thermocouples, embedded thermocouples, radiation pyrometers, metallographic techniques and a method of using powders of constant melting point.

2.2. Numerical Models

Finite element simulations have been successfully applied for modelling orthogonal metal cutting processes. They have significantly reduced the simplifying assumptions of the analytical models. Generally, application of finite element modelling to cutting processes involves two types of formulations; Eulerian or an updated Lagrangian. Moriwaki and Ceretti (1986) [20] presented a further development of Tay's finite element

model and extended its range of application.

Fairweather (1978) [21] presented a finite element solution for the heat transfer problem for the shear plane temperature. They suggested that the band heat source did not move along the shear plane relative to the workpiece as had been assumed by [22]. Moriwaki and Ceretti (1986) [20] developed a thermo-viscoplastic cutting model by using finite element method to analyse the mechanics of steady-state orthogonal cutting process. Validation of the cutting temperature was performed by comparing the simulated temperature distributions, maximum temperature and the location of maximum temperature with Tay et al.'s results and was found in good agreement. The finite element analysis of the orthogonal cutting process conducted by [23] was based on a modified Coulomb's friction model at the tool-chip interface and a stress-based chip separation criterion and the assumption of adiabatic heating conditions. The authors were able to estimate the local temperature rise in the primary and the secondary deformation zones

III.   MATERIALS AND RESEARCH METHODS

Series of experiments were conducted to investigate the temperature distribution in metal cutting operation using carbide cutting tool. The experiment was conducted at Nigerian Machine Tool Osogbo, Osun State.The experimental setup Fig. 2 consists of a constant temperature bath, ice bath, tool-holder voltmeter, k – type thermocouples, D-C power supply and the machine tool. k – type thermocouples were used to measure the transient temperatures. Mercury thermometer was used as the reference temperature when the base is not insulated and when the base is insulated. The results obtained from the experiment were summarized in Tables 1and 2. A typical finite element mesh used in this work is illustrated in Fig.4. The carbide cutting tool was discretized into 183 nodes and 72 elements. Triangular type of element was used. FlexPDE Software was developed to determine the temperatures at the nodal points.

3.1. Experimental Techniques

The technique that was used in the determination of temperature distribution when the carbide cutting tool was not insulated is Tool-Work Thermocouple Technique (Fig. 2). Temperature was measured at the point closer to the hot junction (the contact area between the work piece and carbide cutting tool). The technique that was used in measuring temperature distribution when the carbide cutting tool was insulated is Embedded Thermocouple Technique (Fig. 3). In this method, holes were drilled in the carbide cutting tool that was insulated in order to insert the thermocouple for the measurement of the temperature distribution. `
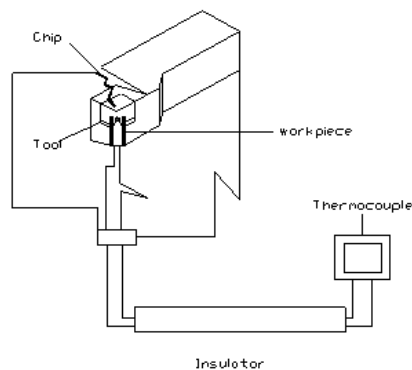

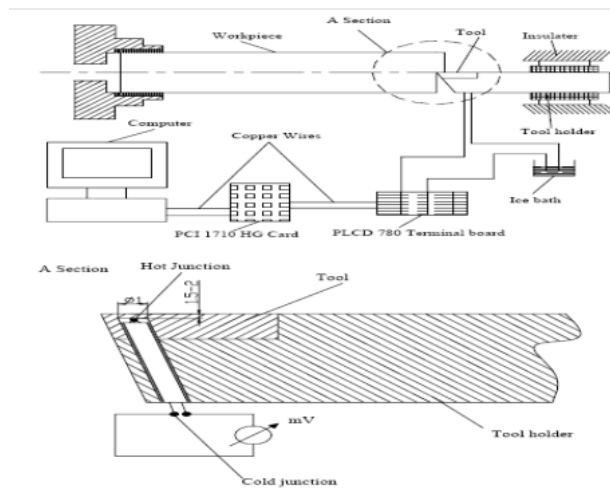**Fig. 2:** The experimental set up of the tool-work thermocouple method

Fig. 3: The experimental set up of the embedded thermocouple method

Fig.4 shows the finite element discretization of the carbide cutting tool where heat is dissipated at the tip of the cutting tool. In this work, triangular sections are taken to allow for the application of the triangular elements in the modeling of the cutting tool. It is assumed that triangular element results with approximate 3-D element results. Hence existing 3-D software is used to solve the model of the cutting tool.
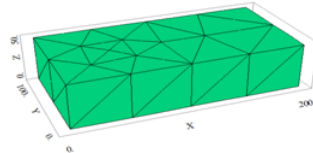

Fig. 4: finite element discretization of the carbide cutting

Table 1: Temperature versus time when the base is not insulated

Time (Sec)	Temperature (^{o}K)
0	297.5
10	297.5
50	297
100	297.5
150	298
200	298
250	298

Table 2: Temperature versus time when the base is insulated

Time (Sec)	Temperature (^{o}K)
0	296.5
10	297
50	305
100	320
150	340
200	365
250	378

IV. FINITE ELEMENT FORMULATION FOR THE HEAT CONDUCTION EQUATION

In many practical machining situations, finding the temperature in a solid body is of vital importance in terms of the maximum allowable temperature, In this study, the derivation of the finite element equations was carried out using Variational method as well as Galerkin method for the three dimensional heat conduction equation. The governing differential equation for the steady state is given as;

$$\frac{\partial}{\partial x}\left(k_x \frac{\partial T}{\partial x}\right) + \frac{\partial}{\partial y}\left(k_y \frac{\partial T}{\partial y}\right) + \frac{\partial}{\partial z}\left(k_z \frac{\partial T}{\partial z}\right) = 0 \tag{1}$$

4.1 Variational Approach

The variational integral, I, corresponding to the above differential equation with its boundary conditions is given by;

$$I(T) = \frac{1}{2}\int_{s_1}\left[k_x\left(\frac{\partial T}{\partial x}\right)^2 + k_y\left(\frac{\partial T}{\partial y}\right)^2 + k_z\left(\frac{\partial T}{\partial x}\right)^2\right]\Omega + \int_{s_2} qTds + \int_{s_3}\frac{1}{2}h\,(T - T_\alpha)^2 \tag{2}$$

The given domain Ω is divided into 'n' number of finite elements with each element having 'r' nodes. The temperature is expressed in each element by;

$$T^e = \sum N_i T_i = (N|T) \tag{3}$$

where $[N] = N_1, N_2, N_3 ...., N_r$ are shape functions and (4) is the vector of nodal temperature, thus;

$$[T] = \begin{bmatrix} T_i \\ T_j \\ \vdots \\ T_\gamma \end{bmatrix} \tag{4}$$

The finite element solution to the problem involves selecting the nodal values of T so as to make the function I (T) stationary. In order to make I (T) stationary, with respect to the nodal values of T, It is required that;

$$\partial I(T) = \sum \frac{\partial T^e}{\partial T_i} = 0 \tag{5}$$

Where n is the total number of discrete values of T assigned to the solution domain. Since T_i is arbitrary, (5) holds true only if;

$$\frac{\partial I}{\partial T_i} = 0 \tag{6}$$

The functional I (T) can be written as a sum of individual functions, defined for the assembly of elements, only if the shape functions giving piece-wise representation of T obey certain continuity and compatibility conditions;

$$I(T) = \sum I^e(T^e) \tag{7}$$

Thus, instead of working with a functional defined over the whole solution region attention is now focused on a functional defined for the individual elements. Hence;

$$\partial I = \sum I^e(T^e) \tag{8}$$

$$\partial I = \sum_{e=1}^{n} \partial I^e = 0 \tag{9}$$

where the variation in I^e is taken only with respect to the r nodal values associated with the element e, that is,

$$\left[\frac{\partial I^e}{\partial T}\right] = \frac{\partial I^e}{\partial T_j} = 0 \quad with\, j = 1,2, ……….r \tag{10}$$

Equation (10) comprises a set of r equations that characterize the behavior of the element e. The fact that we can

represent the functional for the assembly of elements as a sum of the functional for all individual elements provides the key to formulating individual element equations from a variational principle. The complete set of assembled finite element equations for the problem is obtained by adding all the derivatives of I, as given by (10), for all the elements. We can write the complete set of equations as;

$$\frac{\partial I}{\partial T_j} = \sum_{i=1}^{n} \frac{\partial I^e}{\partial T_i} = 0 \qquad with \; i = 1,2, \dots \dots n \qquad (11)$$

The problems are complete when the n set of equations is solved simultaneously for the n nodal values of T. We now give the details for formulating the individual finite element equations from a variational principle.

$$I^e = \frac{1}{2}\int_{\Omega} \left[k_x \left(\frac{\partial T^e}{\partial x}\right)^2 + k_y \left(\frac{\partial T^e}{\partial y}\right)^2 k_z \left(\frac{\partial T^e}{\partial z}\right)^2 - 2GT^e \right] d\Omega + \int_{s_2} qT^e ds + \int_{s_3} \frac{1}{2}h(T^e - \boldsymbol{T_\alpha})^2 \, ds \qquad (12)$$

With

$$T^e = \{N|T\} = [N_1, N_2, \dots N_\gamma] \begin{bmatrix} T_1 \\ T_2 \\ \vdots \\ T_\gamma \end{bmatrix} = N_1 T_1 + N_2 T_2 \dots \dots + N_\gamma T_\gamma \qquad (13)$$

And

$$\frac{\partial T^e}{\partial T_1} = N_1, \qquad \frac{\partial T^e}{\partial T_2} = N_2, \qquad \frac{\partial T^e}{\partial T_\gamma} = N_\gamma \qquad (14)$$

Or
$$\frac{\partial T^e}{\partial [T]} = \begin{bmatrix} N_1 \\ N_2 \\ N_\gamma \end{bmatrix} = [N] = [N]^\gamma \qquad (15)$$

The gradient matrix is written as;

$$[g] = \begin{bmatrix} \frac{\partial T^e}{\partial x} \\ \frac{\partial T^e}{\partial y} \\ \frac{\partial T^e}{\partial z} \end{bmatrix} = \begin{bmatrix} \frac{\partial N_1}{\partial x} \\ \frac{\partial N_1}{\partial y} \\ \frac{\partial N_1}{\partial z} \end{bmatrix} \begin{bmatrix} T_1 \\ T_2 \\ T_\gamma \end{bmatrix} = \{B|T\} \qquad (16)$$

If we consider as follows,

$$[g]^\gamma\{D|g\} = \begin{bmatrix} \frac{\partial T^e}{\partial x} & \frac{\partial T^e}{\partial y} & \frac{\partial T^e}{\partial z} \end{bmatrix} \begin{bmatrix} k & 0 & 0 \\ 0 & k & 0 \\ 0 & 0 & k \end{bmatrix} \begin{bmatrix} \frac{\partial T^e}{\partial x} \\ \frac{\partial T^e}{\partial y} \\ \frac{\partial T^e}{\partial z} \end{bmatrix} = k_x \left(\frac{\partial T^e}{\partial x}\right)^2 + k_y \left(\frac{\partial T^e}{\partial y}\right)^2 + k_z \left(\frac{\partial T^e}{\partial x}\right)^2 \qquad (17)$$

Substituting into equation (14) we have

$$I^e = \frac{1}{2}\int_{\Omega} [(g)^\gamma\{D|g\} - 2GT^e] d\Omega + \int_{s_2} qT^e ds + \int_{s_3} \frac{1}{2}h(T_e - T_\alpha)^2 \, ds \qquad (18)$$

From equation (15) we can substitute $\left[g\right]^T[D]\left[g\right] = [T]^T[B]^T[D][B][T]$ and minimizing the integral, we have (employing (18))

$$\frac{\partial I^e}{\partial [T]} = \int_\Omega \frac{1}{2} 2[[B]^\gamma \langle D|B|T\rangle]\partial\Omega$$

$$-\int_\Omega \frac{1}{2} 2G[N]^\gamma [T]\partial\Omega + \int_{s_{2e}} q[N]^\gamma [T]ds + \int_{s_{3e}} h[N]^\gamma [T]ds - \int_{s_{3e}} h[N]^\gamma T_e ds = 0 \qquad (19)$$

The above equation can be written in a compact form as

$$\{K|T\} = [f] \qquad (20)$$

Where
$$[K] = \int_\Omega [[B]^\gamma \{D|B\}]d\Omega + \int_{s_2} h[N]^\gamma [N]ds \qquad (21)$$

And
$$[f] = \int_\Omega G[N]^\gamma d\Omega - \int_{s_2} q[N]^\gamma ds + \int_{s_2} hT_e[N]^\gamma ds \qquad (22)$$

Equations (20) form the backbone of the calculation method for a finite element analysis of heat conduction problems. It can be easily noted that when there is no heat generation within an element (G= 0), the corresponding term disappears. Similarly, for an insulated boundary (i.e. q = 0 or h = 0) the corresponding term again disappears. In this respect, this is a great deal more convenient as compared to the finite difference method, where nodal equations have to be written for insulated boundaries.

$$[C]\left[\frac{\partial T}{\partial t}\right] + K[T] = [f] \qquad (23)$$

$$C_{ijk}\left[\frac{\partial T_{ijk}}{\partial t}\right] + K_{ijk}[T_i] = [f] \qquad (24)$$

$$[C_{ijk}] = \int_\alpha \ell G N_i dK \qquad (25)$$

$$[C] = \int_\alpha [N]dn \qquad (26)$$

$$f = \int_\alpha G[N]^\gamma dn - \int_\gamma q[N]^\gamma d\sqrt{q} + \int_\gamma hT_\alpha [N]Tdr \qquad (27)$$

As G = 0, then;

$$f = -\int \sqrt{q}\, q[N]^\gamma d\sqrt{q} + \int_\gamma hT_\alpha [N]^\gamma d\gamma \qquad (28)$$

$$[N]^\gamma = [N_i N_j N_k] \qquad (29)$$

$$T = \begin{bmatrix} T_i \\ T_j \\ T_k \end{bmatrix} \qquad (30)$$

$$\frac{\partial T}{\partial t} = \frac{T_n + 1 - T_n}{\Delta t} \qquad (31)$$

$$C\left[\frac{T^{n+1} - T^n}{\Delta t}\right] + K[T^n] = f \qquad (32)$$

$$\frac{C}{\Delta t}[T^{n+1} - T^n] = [f] - K[T^n] \qquad (33)$$

$$C[T^{n+1}] = C[T^n] + \Delta t([f] - K[T^n]) \qquad (34)$$

4.2. The Galerkin's Method

In this subsection, the application of the Galerkin's method for the transient equation subjected to appropriate boundary and initial conditions is addressed. The temperature is discretized over space as follows:

$$T(x, y, z, \tau) = \sum_i^\gamma N_i(x, y, z) T_i(t) \tag{35}$$

where N_i are the shape functions, r is the number of nodes in an element, and $T_i(t)$ are the time-dependent nodal temperatures. The Galerkin representation is given as;

$$\int_\Omega N_i \left[\frac{\partial}{\partial x}\left(K_x(T)\frac{\partial T}{\partial x}\right) + \frac{\partial}{\partial y}\left(K_y(T)\frac{\partial T}{\partial y}\right) + \frac{\partial}{\partial z}\left(K_z(T)\frac{\partial T}{\partial z}\right) - \rho c_\rho \frac{\partial T}{\partial t} \right] d\Omega = 0 \tag{36}$$

Employing integration by parts on the three terms of Equation (47), we get;

$$-\int_\Omega \left[K_x(T)\frac{\partial N_i}{\partial x}\frac{\partial T}{\partial x} + K_y(T)\frac{\partial N_i}{\partial y}\frac{\partial T}{\partial y} + K_z(T)\frac{\partial N_i}{\partial z}\frac{\partial T}{\partial z} - N_i\rho c_\rho \frac{\partial T}{\partial t} \right] d\Omega$$

$$+ \int_{T_{ij}} N_i K_x(T)\frac{\partial T}{\partial x}l dT_{ij} + \int_{T_{ij}} N_i K_y(T)\frac{\partial T}{\partial y}m dT_{ij} + \int_{T_{ij}} N_i K_z(T)\frac{\partial T}{\partial z}n dT_{ij} = 0 \tag{37}$$

Note that from Equation (37)

$$= -\int_{T_{ij}} N_i q dT_{ij} - \int_{T_{ij}} N_i h(T - T_i) dT_{ij} \tag{38}$$

On substituting the spatial approximation from Equation (35), Equation (37) finally becomes;

$$-\int_\Omega \left[K_x(T)\frac{\partial N_i}{\partial x}\frac{\partial T}{\partial x}T_i(t) + K_y(T)\frac{\partial N_i}{\partial y}\frac{\partial T}{\partial y}T_i(t) + K_z(T)\frac{\partial N_i}{\partial z}\frac{\partial T}{\partial z}T_i(t) - N_i\rho c_\rho \frac{\partial T}{\partial t} \right] d\Omega$$

$$+ \int_\Omega \left[-N_i\rho c_\rho \frac{\partial N_i}{\partial t}T_i(t) \right] d\Omega - \int_{T_{ij}} N_i q dT_{ij} - \int_{T_{ij}} N_i h(T - T_\alpha)dT_{ij} = 0 \tag{39}$$

Where i and j represent the nodes, Equation (43) can be written in a convenient form as;

$$[C]\left[\frac{\partial T}{\partial t}\right] + \{K|T\} = [f] \tag{40}$$

$$[C_{ijk}]\left[\frac{\partial T_i}{\partial t}\right] + \{K_{ij}|T_{ij}\} = [f_i] \tag{41}$$

Where

$$[C_{ij}] = \int_\Omega \rho c_\rho N_i N_j d\Omega \tag{42}$$

$$[K_{ij}] = \int_\Omega \left[K_x(T)\frac{\partial N_i}{\partial x}\frac{\partial N_j}{\partial x}(T_i) + K_y(T)\frac{\partial N_i}{\partial y}\frac{\partial N_j}{\partial y}(T_i) + K_z(T)\frac{\partial N_i}{\partial z}\frac{\partial N_j}{\partial z}(T_i) \right] d\Omega + \int_\gamma hN_i N_j dt \tag{43}$$

And

$$[f] = -\int_{\gamma q} qN_i dT_{ij} + \int_{\gamma q} N_i hT_\alpha dT \tag{44}$$

In matrix form,

$$[C] = \int_\Omega \rho c_\rho [N]^T [N] d\Omega \tag{45}$$

And
$$[K] = \int_{\Omega} [B]^T \{D|B\} \, d\Omega + \int_{\gamma} h[N]^T [N] dT \qquad (46)$$

$$[f] = -\int_{\gamma} q[N]^T \, d\gamma + \int_{\gamma} hT_{\alpha} N^T \, d\gamma \qquad (47)$$

For a linear triangular element, the temperature distribution can be written as;
$$T = N_i T_i + N_j T_j + N_k T_k \qquad (48)$$

The thermal conductivity matrix becomes;
$$D = \begin{bmatrix} K & 0 & 0 \\ 0 & K & 0 \\ 0 & 0 & K \end{bmatrix} \qquad (49)$$

The shape functions for a triangular element are given as (Fairweather, 1978), thus;

$$N_i = \left(1 - \frac{x}{3a}\right)\left(1 - \frac{y}{3b}\right)\left(1 - \frac{z}{3c}\right) \qquad (50)$$

$$N_j = \frac{x}{3a}\left(1 - \frac{y}{3b}\right)\left(1 - \frac{z}{3c}\right) \qquad (51)$$

$$N_k = \frac{xyz}{27abc} \qquad (52)$$

But
$$[K] = \int_{\Omega} [B]^T \{D|B\} \, dv + \int_{\gamma} h[N]^T [N] d\gamma \qquad (53)$$

The gradient matrix is given by;

$$g = \begin{bmatrix} \dfrac{\partial T}{\partial x} \\[6pt] \dfrac{\partial T}{\partial y} \\[6pt] \dfrac{\partial T}{\partial z} \end{bmatrix} = \begin{bmatrix} \dfrac{\partial N_i}{\partial x} & \dfrac{\partial N_j}{\partial x} & \dfrac{\partial N_k}{\partial x} \\[6pt] \dfrac{\partial N_i}{\partial y} & \dfrac{\partial N_j}{\partial y} & \dfrac{\partial N_k}{\partial y} \\[6pt] \dfrac{\partial N_i}{\partial z} & \dfrac{\partial N_j}{\partial z} & \dfrac{\partial N_k}{\partial z} \end{bmatrix} \qquad (54)$$

$$B = \begin{bmatrix} \dfrac{\partial N_i}{\partial x} & \dfrac{\partial N_j}{\partial x} & \dfrac{\partial N_k}{\partial x} \\[6pt] \dfrac{\partial N_i}{\partial y} & \dfrac{\partial N_j}{\partial y} & \dfrac{\partial N_k}{\partial y} \\[6pt] \dfrac{\partial N_i}{\partial z} & \dfrac{\partial N_j}{\partial z} & \dfrac{\partial N_k}{\partial z} \end{bmatrix} \qquad (55)$$

4.3. Using the method of Separation of Variables

The three-dimensional transient heat conduction equation is;

$$\frac{\partial^2 T}{\partial x^2} + \frac{\partial^2 T}{\partial y^2} + \frac{\partial^2 T}{\partial z^2} = \frac{1}{\alpha_{\gamma}} \frac{\partial T}{\partial t} \qquad (56)$$

Where α_T is the thermal diffusivity of the material.

Let

$$\theta = \frac{T - T_{\infty}}{T_{\alpha} - T_{\infty}} \qquad (57)$$

The initial condition is: $\qquad \theta(x, y, z, 0) = 1 \qquad (58)$

The boundary conditions for the model when the cutting tool is not insulated are as follows;
 A(i). The heat source is considered as a plane heat source on the top face of the insert with the following

expression.

$$-K\frac{\partial\theta}{\partial x}(x,y,z,t)|_{z=c} = \begin{cases} q_c \ for \ 0 \leq x \leq L_x, 0 \leq y \leq L_y \\ h\theta \qquad\qquad\qquad otherwise \end{cases} \qquad (59)$$
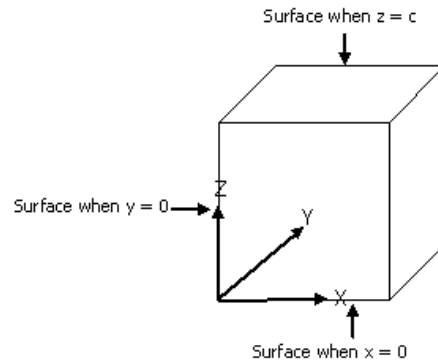
Where q_c is the heat flux flowing into the tool insert.

A(ii). The adiabatic boundary conditions are assumed for the two surfaces which are close to the heat source (x = 0, y = 0) and the bottom surface (z =c) hence;

$$\frac{\partial\theta(0,y,0 \leq z \leq c, \ t)}{\partial x} = 0 \qquad (60)$$

$$\frac{\partial\theta(0,y,0 \leq z \leq c, \ t)}{\partial y} = 0 \qquad (61)$$

$$\frac{\partial\theta(x,y,z,t)}{\partial z}\bigg|_{z=0} = 0 \qquad (62)$$

A(iii). The ambient boundary conditions are assumed for the two surfaces which are at the distance from the heat source (x = a, y = b) can be described as:

$$\theta(a,y,z,t) = 0 \qquad (63)$$

$$\theta(x,b,z,t) = 0 \qquad (64)$$

The boundary conditions for the model with air-cooled are:

B(i). The adiabatic boundary conditions for the two surfaces which are close to the heat source (x=0, y = 0), the bottom surface (z = c) and the surface of insert (x = a, $0 \leq y \leq b$, $0 \leq z \leq c$) which is far away from heat source:

$$\theta(0,y,0 \leq z \leq c,t) = 0 \qquad (65)$$

$$\theta(x,0,0 \leq z \leq c,t) = 0 \qquad (66)$$

$$\theta(x,y,z,t)|_{z=c} = 0 \qquad (67)$$

$$\theta(a,0 \leq y \leq b,0 \leq z \leq c,t) = 0 \qquad (68)$$

Now, by using the method of separation of variables;

$$\frac{\partial^2\theta}{\partial x} + \frac{\partial^2\theta}{\partial y} + \frac{\partial^2\theta}{\partial z} = \frac{1}{\alpha}\frac{\partial\theta}{\partial t} \qquad (69)$$

Let the solution be;

$$\theta(x,y,z,t) = X(x)Y(y)Z(z)T(t) \qquad (70)$$

$$\frac{\partial^2\theta}{\partial x^2} = X^{''}(x)Y(y)Z(z)T(t) \qquad (71)$$

$$\frac{\partial^2 \theta}{\partial y^2} = X(x)Y''(y)Z(z)T(t) \qquad (72)$$

$$\frac{\partial^2 \theta}{\partial z^2} = X(x)Y(y)Z''(z)T(t) \qquad (73)$$

$$\frac{\partial \theta}{\partial t} = X(x)Y(y)Z(z)T'(t) \qquad (74)$$

So,

$$X'(x)Y(y)Z(z)T(t) + X(x)Y'(y)Z(z)T(t) + X(x)Y(y)Z'(z)T(t)$$
$$= \frac{1}{\alpha}X(x)Y(y)Z(z)T'(t) \qquad (75)$$

On dividing through by $X(x)\ Y(y)\ Z(z)\ T(t)$ i.e. equation (70)

We have,

$$\frac{X''(x)}{X(x)} + \frac{Y''(y)}{Y(y)} + \frac{Z''(z)}{Z(z)} = \frac{1}{\alpha}\frac{T'(t)}{T(t)} \qquad (76)$$

$$\frac{X''(x)}{X(x)} = \frac{1}{\alpha}\frac{T'(t)}{T(t)} - \frac{Y''(y)}{Y(y)} - \frac{Z''(z)}{Z(z)} = -\beta^2 \qquad (77)$$

$$\frac{1}{x}\frac{d^2X}{dx^2} = -\beta^2 \qquad (78)$$

$$\frac{d^2X}{dx^2} + \beta^2 X = 0 \qquad (79)$$

Then,

$$X = A\cos\beta x + B\sin\beta x \qquad (80)$$
$$X' = A\beta Sin\beta x + B\beta Cos\beta x \qquad (81)$$
$$X'(0) = A\beta Sin0 + B\beta Cos0 \qquad (82)$$
$$0 = B\beta \qquad hence\ B = 0 \qquad Since\ \beta \neq 0$$

So, on substituting 0 for B, we have;

$$X(x) = ACos\beta x \qquad (83)$$

$$X(\alpha) = ACos\beta\alpha = 0 \qquad (84)$$

$$A \neq 0, \qquad then\ Cos\beta\alpha = 0$$

$$Cos\beta\alpha = Cos\left(\frac{2m-1}{2}\right)\pi = 0 \quad for\ m = 1,2,3\ldots\ldots \qquad (85)$$

$$\beta = \left(\frac{2m-1}{2}\right)\pi \qquad (86)$$

$$X(x) = BCos\left(\frac{2m-1}{2}\right)\pi x \qquad (87)$$

$$\frac{Y''(y)}{Y(y)} = \frac{1}{\alpha}\frac{T'(t)}{T(t)} - \frac{X''(x)}{X(x)} - \frac{Z''(z)}{Z(z)} = -\mu^2 \qquad (88)$$

$$\frac{Y''(y)}{Y(y)} = \frac{1}{\alpha}\frac{T'(t)}{T(t)} - \frac{X''(x)}{X(x)} - \beta^2 = -\mu^2 \qquad (89)$$

$$\frac{Y''}{Y} = -\mu^2 \qquad (90)$$

$$\frac{d^2y}{dy^2} + \mu^2 Y = 0 \qquad (91)$$

$$Y(y) = C\ Cos\mu y + DSin\mu y \qquad (92)$$

$$Y'(y) = -C\mu Sin\mu y + D\mu Cos\mu y \qquad (93)$$

$$Y'(0) = 0 = -CSin0 + D\mu = 0 \qquad (94)$$

$$As\ D\mu = 0 \quad hence\ D = 0$$

Therefore;

$$Y(y) = C \, Cos\mu y \tag{95}$$

$$Y(y) = C \, Cos\mu b = 0 \tag{96}$$

$$C \neq 0 \quad hence \; Cos\mu b = 0$$

$$Cos\mu b = Cos\left(\frac{2n-1}{2}\right)\pi = 0 \qquad for \; n = 1,2,3 \dots \dots \tag{97}$$

$$\mu = \left(\frac{2n-1}{2b}\right)\pi \tag{98}$$

$$\therefore Y(y) = C \, Cos\left(\frac{2n-1}{2b}\right)\pi y \tag{99}$$

$$For \quad \left.\frac{d\theta}{dz}\right|_{z=c} = \frac{qc}{k} \quad and \quad \left.\frac{d\theta}{dz}\right|_{z=0} \tag{100}$$

$$Z(z) = \frac{qc}{k}\left(z - \frac{z^2}{2c}\right) \qquad (Carslaw \; and \; Jaeger, 1989) \tag{101}$$

$$\frac{1}{\alpha T}\frac{dT}{dt} = -(\mu^2 + \beta^2) \tag{102}$$

$$\frac{dT}{Tdt} = -(\mu^2 + \beta^2)\alpha \tag{103}$$

$$\frac{dT}{T} = -(\mu^2 + \beta^2)\alpha dt \tag{104}$$

$$lnT = -(\mu^2 + \beta^2)\alpha t \tag{105}$$

$$\therefore T = \ell^{-(\mu^2+\beta^2)\alpha} = \ell^{-\left[\left(\frac{2m-1}{2a}\right)^2 + \left(\frac{2n-1}{2b}\right)^2 \pi^2 \alpha\right]} \tag{106}$$

Recall

$$\theta\left(x, y, z, T\right) = X(x) \, Y(y) \, Z(z) \, T(t)$$

$$\theta = \sum_{m=1}^{\infty}\sum_{n=1}^{\infty}(AC)\left[Cos\left(\frac{2m-1}{2a}\right)\pi x \, Cos\left(\frac{2n-1}{2b}\right)\pi y \left[\frac{qc}{k}\left(z - \frac{z^2}{2c}\right)\right]\ell^{-\left[\left(\frac{2m-1}{2a}\right)^2 + \left(\frac{2n-1}{2b}\right)^2 \pi^2 \alpha\right]}\right] \tag{107}$$

$$\theta = \sum_{m=1}^{\infty}\sum_{n=1}^{\infty}P_{mn}\left[Cos\left(\frac{2m-1}{2a}\right)\pi x \, Cos\left(\frac{2n-1}{2b}\right)\pi y \left[\frac{qc}{k}\left(z - \frac{z^2}{2c}\right)\right]\ell^{-\left[\left(\frac{2m-1}{2a}\right)^2 + \left(\frac{2n-1}{2b}\right)^2 \pi^2 \alpha\right]}\right] \tag{108}$$

$$\theta = \frac{qc}{k}\left[\sum_{m=1}^{\infty}\sum_{n=1}^{\infty}P_{mn} \, Cos\left(\frac{2m-1}{2a}\right)\pi x \, Cos\left(\frac{2n-1}{2b}\right)\pi y \left(z - \frac{z^2}{2c}\right) \ell^{-\left[\left(\frac{2m-1}{2a}\right)^2 + \left(\frac{2n-1}{2b}\right)^2 \pi^2 \alpha\right]}\right] \tag{109}$$

$$\theta = \frac{qc}{k}\left(z - \frac{z^2}{2c}\right)\sum_{m=1}^{\infty}\sum_{n=1}^{\infty}P_{mn}\left[Cos\left(\frac{2m-1}{2a}\right)\pi x \, Cos\left(\frac{2n-1}{2b}\right)\pi y \, \ell^{-\left[\left(\frac{2m-1}{2a}\right)^2 + \left(\frac{2n-1}{2b}\right)^2 \pi^2 \alpha\right]}\right] \tag{110}$$

Also recall,

$$\theta = \frac{T - T_\infty}{T_o = T_\infty} \quad at \; t = 0, \; T = T_0 \; hence \; \theta = 1$$

$$1 = \frac{qc}{k}\left(z - \frac{z^2}{2c}\right)\sum_{m=1}^{\infty}\sum_{n=1}^{\infty}P_{mn}\left[Cos\left(\frac{2m-1}{2a}\right)\pi x \, Cos\left(\frac{2n-1}{2b}\right)\pi y\right] \tag{111}$$

$$P_{mn} = \int_0^a\int_0^b\left[Cos\left(\frac{2m-1}{2a}\right)\pi x \, Cos\left(\frac{2n-1}{2b}\right)\pi y\right]dxdy = \frac{4ab(-1)^{m+n}}{(2m-1)(2n-1)\pi^2} \tag{112}$$

Therefore,

$$\theta = \frac{qc\left(z - \frac{z^2}{2c}\right)}{k\pi^2} \sum_{m=1}^{\infty} \sum_{n=1}^{\infty} \left[\frac{4ab(-1)^{m+n}}{(2m-1)(2n-1)\pi^2} Cos\left(\frac{2m-1}{2a}\right)\pi x \ Cos\left(\frac{2n-1}{2b}\right)\pi y \ \ell^{-\left[\left(\frac{2m-1}{2a}\right)^2 + \left(\frac{2n-1}{2b}\right)^2 \pi^2 \alpha\right]} \right] \quad (113)$$

The above equation was simulated by MatLab 7.5 and the results obtained are shown in the figures below. Also the following data was employed in the finite element simulation: Width, a = 50mm, Length, b = 50mm, Thickness, c = 20mm, Thermal Conductivity = 120W/mK, Density = 7800Kg/m^2, Specific Heat = 343.3J/KgK, Initial Temperature = 298K, q_c = 8.125x10^6 W/m^2

Subject to the following boundary conditions: At, x = 25mm, y = 100mm, z = 50mm, T = 298K, and
At, x = 38.74068mm, y = 38.74068mm, z = 50mm, T= 404.7755K.
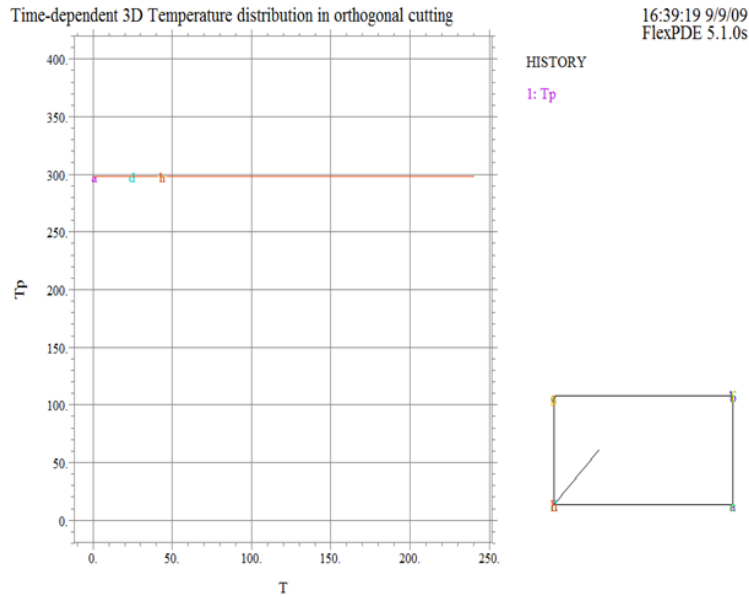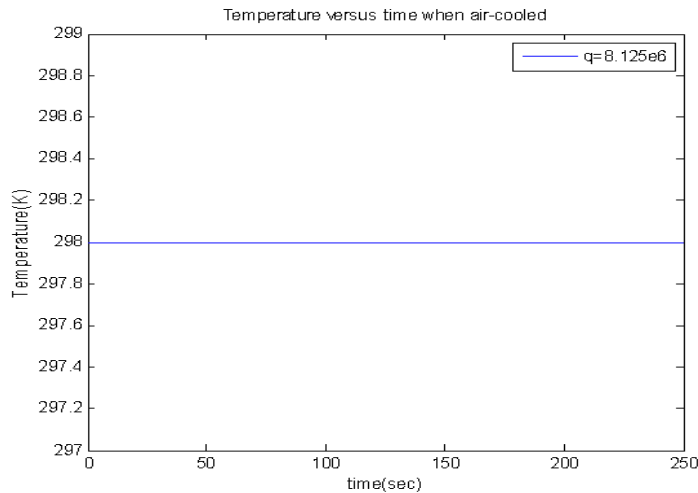
V. RESULTS OF ANALYSIS AND SIMULATION

Fig. 5: The temperature distribution against time on the cutting tool when the base is convecting

Fig. 5 shows that when the carbide cutting tool was air-cooled, it maintained constant temperature of 298K. This result agreed with the results obtained analytically and experimentally.

ig. 6 shows result obtained analytically, it was shown that when the carbide cutting tool was air-cooled, it maintained constant temperature of 298K. This agrees with the result of FEM and the result obtained experimentally.
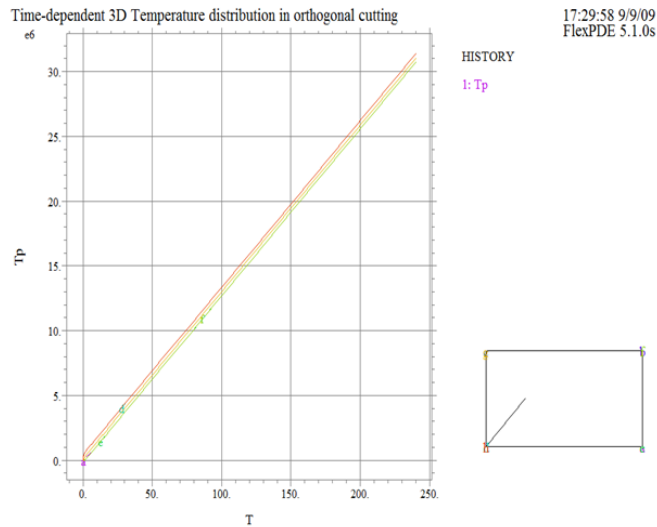

Fig. 7: The temperature distribution against time on the cutting tool when the base is insulated

Fig. 7 shows that when carbide cutting tool was insulated, the temperature increases rapidly. The result agrees with the result obtained analytically and experimentally.
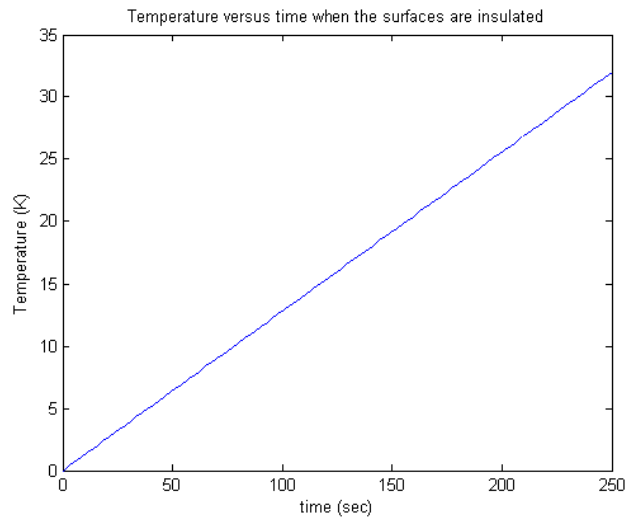

Fig. 8: Analytical result of the temperature distribution in metal cutting when the base is insulated

Fig. 8 shows the analytical result for the insulated carbide cutting tool. It was revealed that when the carbide cutting tool was insulated, the temperature increases rapidly. The above result agrees with FEM result and the result obtained experimentally.
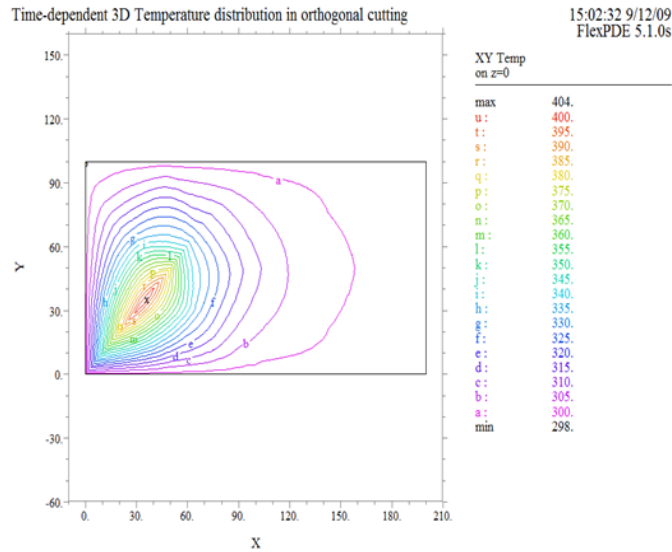
Fig. 9: FEM analysis of the temperature distribution on the carbide cutting tool when the base is

convecting

From the results obtained in FEM analysis as shown in Fig. 9, it was observed that the maximum temperature is 404K and the minimum temperature is 298K. The temperature at any point can be deducted from the results above. Therefore, the temperature at the tip of the cutting tool is higher than that far away from the cutting tool.
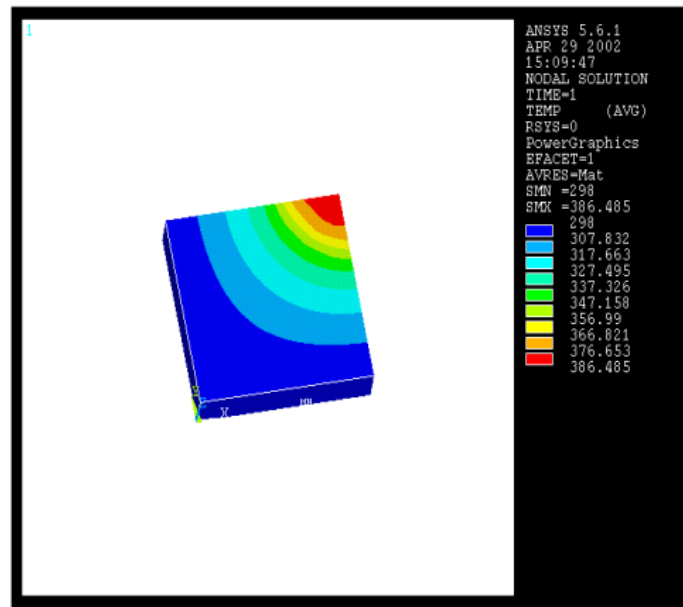

Fig. 10: ANSYS simulation of the temperature distribution on the cutting tool

The ANSY results of Fig. 10 agree with the results obtained in FEM analysis. It has a maximum temperature of 386.485K at the tip of the carbide cutting tool and the minimum temperature is 298K.
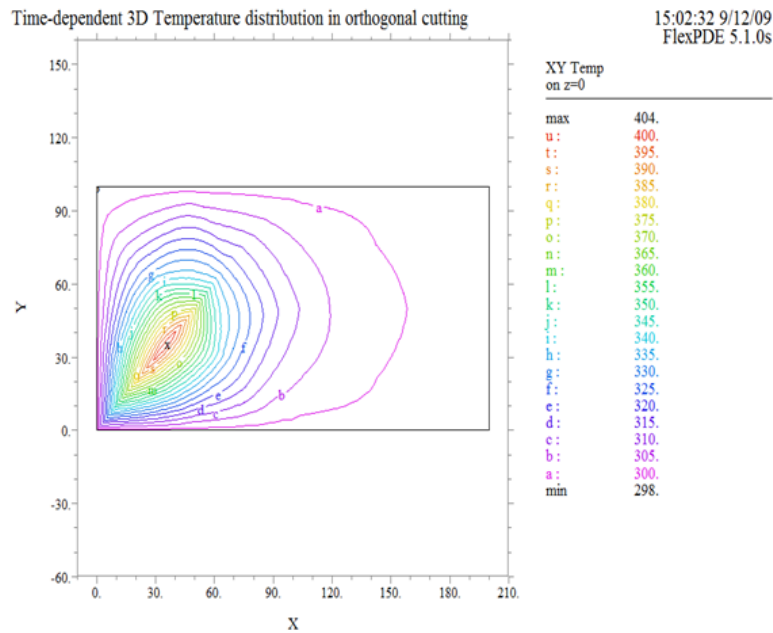
Fig.11: FEM analysis of the temperature distribution on the cutting tool when the base is insulated

The maximum temperature of the carbide cutting tool when it was insulated is 404K and the minimum temperature is 298K
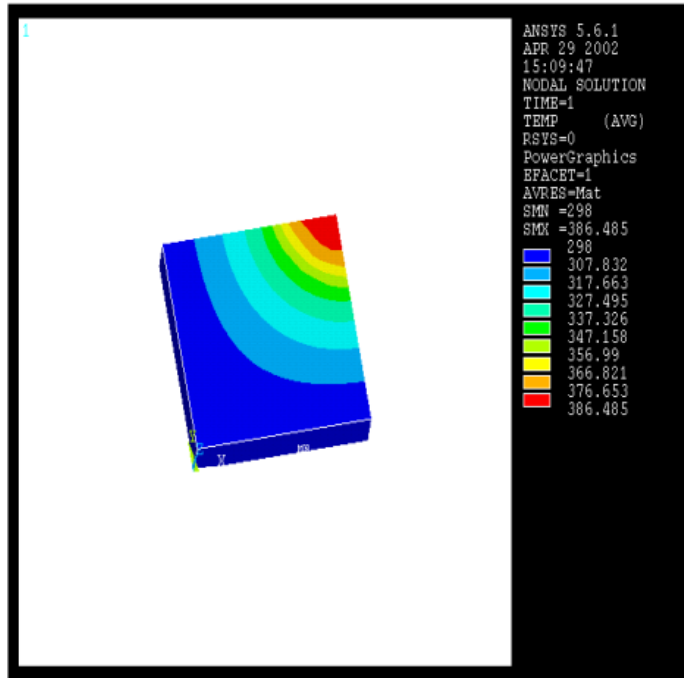

Fig. 12: ANSYS simulation of the temperature distribution on the cutting tool

The maximum temperature obtained from ANSYS simulation when the carbide cutting tool was insulated is 386.485K and the minimum temperature is 298K.

VI.   CONCLUSION

The temperature distributions of carbide cutting were plotted in Figs. 5-12 comparing boundary conditions and cooling effects. It was noted that the air-cooled effects on the heat flux of both heat sources are rather minor. Thus, it can be concluded that the air cooled method does not alter the chip formation process. Further, the simulation results of boundary conditions and coolants were done to see the effects on the cutting tool with the analytical results. The results generated from Finite Element Method and analytical method revealed that the cutting tip maintained a constant atmospheric temperature when the cutting tool is efficiently air-cooled but the temperature increases rapidly when the tool is subjected to adiabatic boundary conditions. The simulated numerical and analytical results reasonably agree with the experimental results obtained from ANSYS. The models can be used to investigate the effects of the major parameters on the cooling efficiency. Without involving intensive computation for chip formation analysis, this study used the derived heat-source characteristics as the input of temperature simulations.

REFERENCES

[1].   Balaji, A. K., Sreeram, G., Jawahir, I. S., and Lenz, E., (1999), 'The Effect of Cutting Tool Thermal Conductivity on Tool-Chip Contact Length and Cyclic Formation in Machining with Grooved Tools,' animals of the CIRP, Vol. 48, pp. 33-38.
[2].   Kalpakjian, Serope and Schmid, Steven, R.,(2001)."Manufacturing Engineering and Technology-4th Editon" 34:109-124.
[3].   [3] Barrow, G.A. (1973). Review of Experimental and Theoretical Techniques for Assessing Cutting Temperatures. Annals of the College International pour la Recherche en Productique (CIRP), 22(2):203–211.
[4].   aran, H. and Thuvander, A., (1998), "Modeling Tool Stresses and Temperature Evaluation in Turning Using Finite Element Method ," Machining Science and Technology, Vol. 2, pp. 355-367.
[5].   Jen, Tien-Chien and Anagonye, Aloysius U., 2001, "An Improved Transient Model of Tool Temperatures in etal Cutting," Transactions of ASME, Journal of Manufacturing Cutting, Vol. 123, pp. 321-343.
[6].   Maekawa, Katsuhiro, nakano, Yoshihiro and Kitagawa, takeaki, (1996) "Finite Element Analysis of Thermal Behavior iv Metal Cutting," JSME International Journal, series C, Vol. 39 No. 4 pp. 864-869.
[7].   Tay, A.O., Stevenson, M.G., and de Vahl Davis, G. (1974). Using the Finite Element Method to Determine Temperature Distributions in Orthogonal Machining. Proceedings of the Institution of Mechanical Engineers, part1 188:627–638.
[8].   Usui, E., Shirakash, T. and Kitagawa, T., (1978), "Analytical Pridiction of Three-Dimensional Cutting Process Part 3, Cutting Temperature and Crater Wear of Carbide Tool," ASME Journal of Engineering for Industry, Vol. 100, pp.236-243.
[9].   Radulescu, R. and Kapoor, S. G., (1994) "An Analytical Model for Pridiction of Tool Temperaure Fields during Continuos and Interrupted Cutting," Transactions of the ASME, Journal of Engineering for Industry, Vol.116, pp. 135-143.
[10].   0 Chiou, Richard Y., Chen, Jim S-J., Cooper, Derrek, and Ciuciu, Cristian, (2000), "Environmentally Conscious Investigation of Cutting Fluid Mist Behaviour via Particle Image Veocimetry in Turning," ASME International Mechanical Engineering Conference and Exposition, Vol. 11, pp. 829-834.
[11].   Hahn, R.S. (1951). On the Temperature Developed at the Shear Plane in the Metal Cutting Process. Proc. of irst U.S. National Congress of Applied Mechanics, 661–666.
[12].   [12] Trigger, K.J. and Chao, B.T. (1958). An Analytical Evaluation of Metal Cutting Temperatures. Transactions of the ASME, 73:57–68.
[13].   Komanduri, R. and Hou, Z.B. (2001). Thermal Modeling of the Metal Cutting Process, Part 2: Temperature Rise Distribution Due to Frictional Heat Source at the Tool-chip Interface.International Journal of Mechanical Sciences, 43:57–88.
[14].   Jaeger, J.C. (1992). Moving Sources of Heat and the Temperatures at Sliding Contacts. Proceedings Royal Society of NSW, 76:203–
[15].   Outeiro, J.C., Dias, A.M. and Lebrun, J.L. (2004) 'Experimental assessment of temperature distribution in three-dimensional cutting process', Machining Science and Technology, Vol. 8,No. 3, pp.357–376.
[16].   Silva, M.B. and Wallbank, J. (1999). Cutting Temperature: Prediction and Measurement Methods— A Review. Journal of Materials Processing Technology, 88:195–202.
[17].   Sullivan, D. and Cotterell, M. (2001) 'Temperature measurement in single turning point',Journal of Materials Processing and Technology, Vol. 118, pp.301–308.
[18].   9] Sutter, G., Faure, L., Molinari, A., Ranc, N. and Pina, V. (2003) 'An experimental technique for the measurement of temperature fields for the orthogonal cutting in high speed', International Journal of Machines Tools and Manufacture, Vol. 43, pp.671–678.
[19].   L. (1986) Using Finite Element method to Determine Temperature in Orthogonal Machining. Institution of Mechanical Engineers, 124:304-358.
[20].   Fairweather, G. (1978) 'Finite element Galerkin Methods for Differential Equations'. New York.
[21].   Stephenson, K.,Lowewen, C.and Show, G. (1984) Finite Element Method to Determine Temperature in Orthogonal Machining. ASME Journal of Engineers for Industry. 62:148-172.
[22].   Tay, A.O., Stevenson, M.G., and de Vahl Davis, G. (1997). Using the Finite Element Method to Determine Temperature Distributions in Orthogonal Machining. Proceedings of the Institution of Mechanical Engineers, part 2,113:58-112.